(42) M. Iwata, K. Nakatzu, and Y. Saito, *Acta Crystallogr., Sect. B*, **25**, 2562 (1969).
(43) K. Nakatsu, Y. Saito, and H. Kuroya, *Bull. Chem. Soc. Jpn.*, **29**, 428 (1956).
(44) J. H. Enemark, M. S. Quinby, L. L. Reed, M. J. Steuck, and K. K. Walthers, *Inorg. Chem.*, **9**, 2397 (1970).
(45) D. J. Hodgson, P. K. Hale, and W. E. Hatfield, *Inorg. Chem.*, **10**, 1061 (1971).

Contribution from the Laboratoire de Chimie des Métaux de Transition and Laboratoire de Spectrochimie du Solide,
Université Pierre et Marie Curie, 75230 Paris Cedex 05, France

Structure and Properties of the Mixed-Valence $[W_4O_8Cl_8(H_2O)_4]^{2-}$ Ion

YVES JEANNIN,*[1] JEAN-PIERRE LAUNAY,[1] JACQUES LIVAGE,[2] and ALEXANDRA NEL[1]

Received May 5, 1977

The crystal structure of the mixed-valence W^V/W^{VI} salt $[HNMe_3]_2[W_4O_8Cl_8(H_2O)_4]\cdot 2H_2O$ has been determined from three-dimensional x-ray data collected by counter techniques with Mo Kα radiation. The structure was refined by full-matrix least-squares methods, using 833 observed independent reflections, to a conventional weighted R factor of 0.034. Crystal data are as follows: orthorhombic, space group *Ccca*, $a = 11.42$ (1) Å, $b = 22.84$ (1) Å, $c = 11.80$ (1) Å, $Z = 4$. The $W_4O_8Cl_8(H_2O)_4^{2-}$ ion is formed by the association of four $WO_3Cl_2(H_2O)$ octahedra sharing corners. The four W atoms form a nearly planar square and are joined through linear oxygen bridges. Each W atom is displaced toward a terminal unshared oxygen atom and is thus found alternately 0.18 Å above or below the molecular plane. Although metal atoms are crystallographically equivalent, the complex must be considered as containing 2 W^V and 2 W^{VI}, as shown by ESCA and especially ESR studies. The latter technique reveals the existence of an intramolecular electronic exchange (hopping) occurring at a rate of ca. 10^8 Hz at −50 °C. The electronic spectrum is also discussed.

Introduction

Mixed-valence compounds contain ions of the same element in different formal oxidation states.[3,4] This yields new properties which may not be the sum of those due to the isolated constituents in their pure oxidation states; in particular, magnetic and optical behavior, as well as electronic conductivity, can be drastically modified.

Robin and Day[3] proposed a classification of these compounds, according to the more or less delocalized character of valence electrons. Class I includes those compounds in which valences are so firmly trapped that no interaction occurs and their properties are just the sum of the properties of their components. On the other hand, class III compounds exhibit a complete delocalization of valence electrons via polycentric molecular orbitals, and no integer oxidation states can be ascribed to the constitutive metal ions. Intermediate cases are referred to as class II, where there is only a slight delocalization in the ground state, and, as a first approximation, different integral oxidation states can be ascribed to the constitutive elements. However, a valence exchange can occur through two mechanisms:[5] (i) by light absorption, generally in the visible part of the spectrum (intervalence transfer absorption) and (ii) by thermal exchange which constitutes an internal homonuclear redox reaction (hopping).

The distinction between class II and III mixed-valence complexes is commonly based upon the existence or nonexistence of distortions of the metal–ligand bonds induced by the change in the oxidation state.[6,7] In class II compounds, these distortions are present; for instance, metal–ligand distances are longer for the lower oxidation state, and the valence electrons are thus self-trapped since metallic sites are no longer equivalent. On the contrary, for class III compounds, all sites are strictly equivalent giving rise to a full delocalization of the valence electrons.

A number of mixed-valence compounds can be obtained from molybdenum or tungsten, especially between oxidation state V and oxidation state VI. A mixed anion, formulated as $W_4O_8Cl_8^{2-}$ with formally 2 W^V and 2 W^{VI}, has been prepared by one of us.[8] It can be obtained upon addition of sodium tungstate to a concentrated solution of W^V in 8–12 M HCl. Reaction 1 occurs, the equilibrium being displaced

$$2WO_2Cl_4^{2-} + 2WOCl_5^{2-} + 2H_2O \leftrightharpoons W_4O_8Cl_8^{2-} + 4H^+ + 10Cl^- \quad (1)$$

toward the left. However, by means of selective precipitation, the mixed-valence compound can be obtained free from its constituents.

This paper deals with structural and spectroscopic studies of the trimethylammonium salt $[W_4O_8Cl_8(H_2O)_4](HNMe_3)_2\cdot 2H_2O$. The pyridinium salt, which was isolated and crystallized first, appeared to be unsuitable for an x-ray structural determination, presumably as a result of crystallographic disorder.

Experimental Section

Preparation of Crystals. A ca. 0.15 M W^V solution in 12 M HCl was prepared according to a method already described.[8] W^{VI} was then added as powdered $Na_2WO_4\cdot 2H_2O$ in stoichiometric amount, with vigorous stirring. The reaction mixture was kept at 0 °C for 2–3 days, in order to shift the equilibrium toward the right.[8] A mixture of blue oxides and sodium chloride precipitated and was filtered off. The addition of trimethylammonium chloride at ca. 0.02 M concentration to the dark blue solution gave rise to a slow (1 day) crystallization.

As an alternative procedure, trimethylammonium chloride was added at a 0.04 M final concentration to the W^V solution. The mixture was slowly oxidized by atmospheric oxygen, for instance, by keeping it in a loosely stoppered flask. The W^V–W^{VI} complex slowly appeared as crystals after a few days. Anal. Calcd for $[W_4O_8Cl_8(H_2O)_4][HN(CH_3)_3]_2\cdot 2H_2O$: W, 53.48; Cl, 20.62; C, 5.23; N, 2.03. Found: W, 52.59; Cl, 20.67; C, 5.14; N, 2.02.

X-Ray Studies. The crystals were in the form of tangled tablets but monocrystalline samples could be obtained by cleavage. A trapezoidal-based prism was set in a Pyrex tube with its 101 axis along the rotation axis and sealed under argon, the x-ray path length ranging from 0.25 to 0.1 mm.

The unit cell was found orthorhombic by the precession method using Mo Kα radiation (0.71069 Å). Lattice constants were measured on films, using a binocular with micrometric film translations. Cell parameters obtained were $a = 11.42$ (1) Å, $b = 22.84$ (1) Å, and $c = 11.80$ (1) Å.

Systematic extinctions, $h + k = 2n$ for all reflections, $l = 2n$ for $0kl$ and $h0l$, and $h = 2n$ for $hk0$, unambiguously designated the space

0020-1669/78/1317-0374$01.00/0

Table I. Final Positional and Thermal Parameters[a,b]

Atom	x	y	z	$10^4\beta_1$	$10^4\beta_2$	$10^4\beta_3$	$10^4\beta_4$	$10^4\beta_5$	$10^4\beta_6$
W	−0.01635 (4)	0.16917 (3)	0.09314 (5)	36.8 (5)	13.4 (1)	26.8 (4)	−0.4 (2)	1.2 (4)	1.9 (2)
Cl1	0.0246 (4)	0.0667 (1)	0.0913 (5)	85 (4)	17 (1)	73 (3)	−1 (1)	13 (4)	−8 (1)
Cl2	0.0241 (3)	0.1648 (2)	−0.1063 (3)	76 (3)	23 (1)	32 (3)	−2 (2)	8 (3)	−2 (1)
O1	−0.1649 (7)	0.1638 (7)	0.080 (1)	25 (7)	38 (4)	69 (10)	0 (5)	9 (7)	−1 (7)
O2	0.1833 (8)	0.1735 (7)	0.103 (1)	42 (7)	34 (3)	42 (9)	−5 (5)	19 (7)	4 (6)
O3	0	0.25	0.089 (1)	106 (15)	7 (3)	60 (11)	−2 (6)	0	0
O4	0	0.1683 (8)	0.25	64 (12)	21 (3)	20 (11)	0	0 (9)	0
O5	−0.294 (1)	0.25	0.25	51 (13)	26 (4)	43 (10)	0	0	8 (9)

Atom	x	y	z	B, Å^2	Atom	x	y	z	B, Å^2
N	−0.217 (2)	0.015 (1)	0.205 (2)	4.1 (6)[c]	C2	−0.254 (6)	0.013 (2)	0.079 (4)	6 (1)[c]
C1	−0.302 (4)	0.045 (2)	0.284 (5)	4 (1)[c]	C3	−0.179 (6)	−0.043 (3)	0.248 (9)	7 (2)[c]

[a] Estimated standard deviations in parentheses referring to the last digit. [b] Anisotropic temperature factors are defined by $\exp[-h^2\beta_1 - k^2\beta_2 - l^2\beta_3 - 2hk\beta_4 - 2hl\beta_5 - 2kl\beta_6]$. [c] Isotropic temperature factor.

group *Ccca*. The calculated density of 2.69 g cm^{-3} for 4 formula units per unit cell agrees with the experimental density of 2.92 g cm^{-3} measured by the flotation method in a mixture of $C_2H_2Br_4$ and C_2H_5I.

Intensity measurements have been carried out on a four-circle automatic diffractometer with Mo Kα radiation. A takeoff angle of 2° was used. The crystal focus distance was 225 mm and the crystal counter distance was 235 mm. Intensities were measured at room temperature with a scintillation counter and a pulse-height analyzer set on Mo Kα energy in such a way that 90% of the diffracted intensity was collected. A graphite monochromator was set in front of the counter window.

There were 957 independent reflections collected with Bragg angles of less than 22° of which 124 were null. The θ–2θ scan technique was used with a scan rate of 1° min^{-1} in Bragg angle; the Kα dispersion was taken into account. Background intensity was measured during 15 s before and after each scan, in fixed positions. Three reference reflections were monitored every 50 reflections and found to be constant. All intensities were corrected for counting losses[9] and for Lorentz polarization factors.

For each reflection, the statistical error ERR on integrated intensity was computed as

$$\mathrm{ERR} = \left[I(\mathrm{obsd}) + \mathrm{CORPER} + \mathrm{FC}\left(\frac{\mathrm{BAL}}{\mathrm{TFC}}\right)^2\right]^{1/2}$$

in which I(obsd) is the observed intensity, CORPER is the counting loss, FC is the background count, BAL is the sweep time, and TFC is the duration of the background count. The standard deviation was taken as $\sigma = \mathrm{ERR}/2F$ (F being the structure factor) for nonzero reflections and $\sigma = (\mathrm{ERR}/3)^{1/2}$ for null reflections.

Atomic parameters have been refined using a full-matrix least-squares program. The quantity minimized was $\sum w^2(|F_o| - |F_c|)^2$, where F_o and F_c are the observed and calculated structure factors put on the same scale and w are weights taken as $1/\sigma$. R factors are defined by $R = \sum(|F_o| - |F_c|)/\sum|F_o|$ and $R_w = [\sum w^2(|F_o| - |F_c|)^2/\sum w^2|F_o|^2]^{1/2}$. Atomic scattering factors were those published by Cromer and Waber[10a] and were corrected for the real and imaginary parts of anomalous dispersion for tungsten and chlorine, $\Delta f'$ and $\Delta f''$ being taken from ref 10b. Absorption correction has been carried out with the ORABS program.[11] The linear absorption coefficient was 168 cm^{-1} and the transmission coefficient ranged from 0.203 to 0.036.

Solution and Refinement of Structure. The position of the unique crystallographically independent tungsten atom was readily determined from a three-dimensional Patterson synthesis. A subsequent Fourier map revealed the chlorine atoms as well as two oxygen atoms O1 and O2. At this stage, R_w was 0.190 but dropped to 0.108 after absorption correction. A new Fourier map located the remaining oxygen atoms (O3, O4, and O5). Carbon and nitrogen atoms were then found from Fourier difference maps in general positions, indicating a statistical distribution of the cation with an occupancy factor of 0.5. No features allowing hydrogen atom localization were present in the final difference map. In final cycles all atoms were refined with anisotropic temperature factors, except N, C1, C2, and C3 for which an isotropic temperature factor was used. After exclusion of two obviously erroneous reflection measurements, R_w was equal to 0.059. The correction for secondary extinction was necessary since it led to a significative lowering in R_w. The final R values were as follows: unweighted R = 0.047 (including zeros) or 0.038 (excluding zeros); weighted R_w = 0.034 (including zeros) or 0.033 (excluding zeros). The secondary extinction parameter was 1.0×10^{-7}. The quantity (F_{000})(SC) in which SC is the scale factor was 1342. All refinements were carried out by inverting the full normal-equation matrix.

Table II. Interatomic Distances and Angles[a]

	Distances, Å		
W–Cl1	2.389 (5)	W–W, along b	3.721 (2)
W–Cl2	2.406 (5)	W–W, along c	3.735 (2)
W–O1	1.711 (9)		
W–O2	2.29 (1)	N–C1	1.49 (6)
W–O3	1.856 (1)	N–C2	1.55 (5)
W–O4	1.860 (2)	N–C3	1.49 (9)
	Angles, Deg		
W–O3–W	177 (2)	O4–W–O3	91.5 (8)
W–O4–W	179 (2)	Cl2–W–O1	95.7 (6)
Cl1–W–Cl2	84.9 (2)	Cl2–W–O2	82.1 (4)
Cl1–W–O1	97.0 (7)	Cl2–W–O3	89.9 (6)
Cl1–W–O2	81.2 (5)	O3–W–O1	99.9 (7)
Cl1–W–O3	162.7 (1)	O3–W–O2	81.7 (5)
Cl1–W–O4	88.7 (6)	O1–W–O2	177.3 (7)
O4–W–O2	81.1 (3)		
O4–W–Cl2	162.8 (2)	C1–N–C2	115 (4)
O4–W–O1	100.9 (5)	C1–N–C3	114 (6)
		C2–N–C3	114 (6)

[a] See Figure 2 for labeling.

Atomic parameters with their estimated standard deviations are collected in Table I. Interatomic distances and angles are shown in Table II.

ESCA Measurements. X-ray photoelectron spectra were measured with an AEI spectrometer, Type ES 200B, operating with a Mg Kα radiation (1253.6 eV). Binding energies have been obtained by assigning 285.0 eV to the C(1s) line. The powdered samples were pressed on a copper grid and transferred into the spectrometer. The residual pressure was about 10^{-8} Torr.

Electron Spin Resonance. ESR spectra were recorded on a Jeol X-band spectrometer, with a TE_{011}-mode cylindrical cavity. Experiments at 77 K were made in a quartz Dewar, containing liquid nitrogen, inserted into the cavity. Low temperatures, between 130 and 300 K, were obtained by blowing cold nitrogen gas through the cavity. The magnetic field was measured with a proton NMR probe and the microwave frequency with a wavemeter giving an accuracy of ±1 MHz.

Electronic Spectrum. The electronic spectrum was recorded with a Beckman DK 2A spectrophotometer, immediately after dissolution of the trimethylammonium salt in 12 M HCl at 0 °C. Under these conditions, the decomposition of the $W_4O_8Cl_8(H_2O)_4^{2-}$ ion could be neglected. The same spectrum was observed in acetonitrile.

Results and Discussion

Crystal Structure. The structure is made of discrete $W_4O_8Cl_8(H_2O)_4^{2-}$ and $HNMe_3^+$ ions. The four tungsten atoms of each anion form a roughly planar square, perpendicular to the a axis. Anions alternately lie at x = 0 and x = 0.5 levels (see Figure 1) and cations are found between them

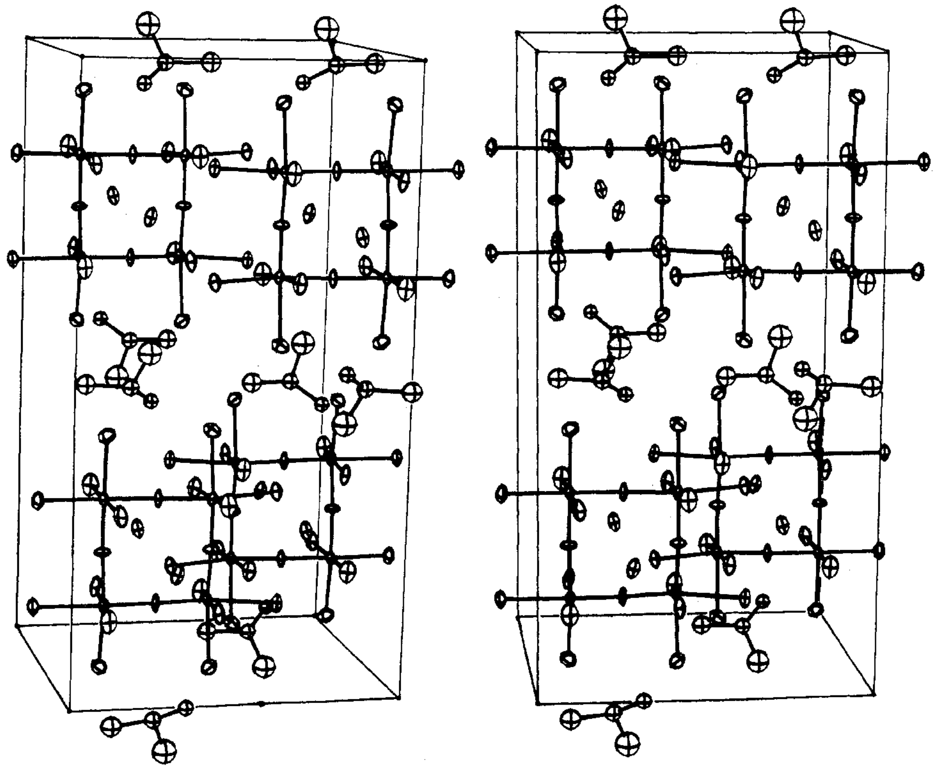

Figure 1. Stereoscopic view of the unit cell. Thermal ellipsoids are shown at the 25% probability level. An arbitrary orientation has been selected for the trimethylammonium cation.

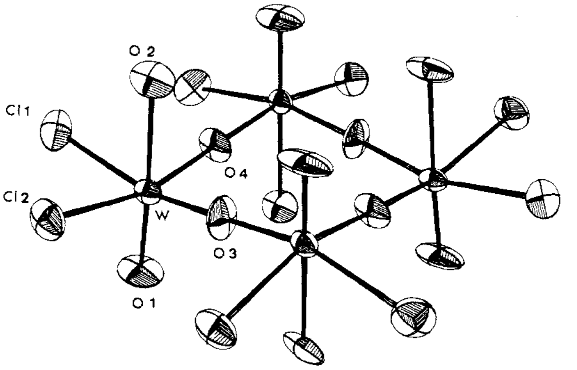

Figure 2. ORTEP drawing of the $W_4O_8Cl_8(H_2O)_4^{2-}$ ion. Thermal ellipsoids are shown at the 50% probability level.

at $x \simeq 0.25$ and $x \simeq 0.75$ intermediate levels. In addition, eight water molecules per unit cell are found in special positions (O5 in Table I); their oxygen atoms are located exactly above the center of a W_4 square ($y = z = 0.25$).

The nitrogen and carbon atoms of the cation are found in general positions with an occupancy factor of 0.5. They lie near a C_2 axis which crosses the trimethylammonium cation; the orientation of the whole cation is thus statistically disordered.

The $W_4O_8Cl_8(H_2O)_4^{2-}$ ion is shown[12] in Figure 2. The structure can be described as four $WO_3Cl_2(H_2O)$ octahedra sharing corners in such a way that the W atoms are in a roughly square arrangement. This building is formally analogous to the association of four octahedra in NbF_5 or TaF_5.[13] All tungsten atoms are crystallographically equivalent.

The interatomic distances and bond angles (see Table II) show that the tungsten atom is not at the center of its octahedron. Thus the square is not strictly planar, the tungsten atoms being alternately 0.18 Å above or below the molecular plane. The tungsten-tungsten distances corresponding to the edges of the square are so close (3.72 and 3.73 Å) that the molecule can be considered as belonging to the D_{2d} point group.

Table III. Correlation between the W-O Bridging Distance and the W-O-W Bridge Angle

Compd	Angle, deg	Dist, Å	Ref
$K_4[SiW_{12}O_{40}]\cdot 17H_2O$	121	1.96	16
	150	1.91	
$(HNMe_3)_2[W_4O_8Cl_8(H_2O)_4]\cdot 2H_2O$	180	1.86	This work
$K_4[W_2OCl_{10}]$	180	1.87	17

The particularly long W-O2 distance is characteristic of a coordinated water molecule; for instance, the Mo-OH_2 distance is 2.34 Å in $MoOCl_4(H_2O)^-$.[14] On the contrary, the W-O1 distance is particularly short (1.71 Å) and is indicative of strong π character as usual for oxotungsten groups. The marked distortion with respect to octahedral coordination is also usual in the chemistry of tungsten (see for instance the structures of heteropolyanions[15]). W-O3 and W-O4 distances are rather short and indicate some π character in W-O-W bridges. A valuable comparison can be made with metal-bridging oxygen distances in heteropolyanion structures. Indeed, accurate neutron diffraction measurements have been carried out by Smith on $K_4SiW_{12}O_{40}\cdot 17H_2O$.[16] A correlation then appears between the W-O bridging distance and the W-O-W bridge angle (Table III). We have also mentioned the distance obtained by Jezowska-Trzebiatowska et al.[17] for the linear $[Cl_5W^{IV}\text{-}O\text{-}W^{IV}Cl_5]^{4-}$ ion which is very close to our value, despite the fact that tungsten is in a different oxidation state. The decrease in the W-O distance when the bridge angle approaches 180° is characteristic of the existence of metal-oxygen π bonds. An analogous correlation is observed for various bichromates.[18] This π character of the linear W-O-W chain allows an easy electronic exchange between two neighboring tungsten atoms.

ESCA Spectrum. The x-ray photoelectron spectrum of the trimethylammonium salt is shown on Figure 3 in the region of W(4f) core electrons. A complex signal is observed which cannot be explained by a single oxidation state for tungsten.

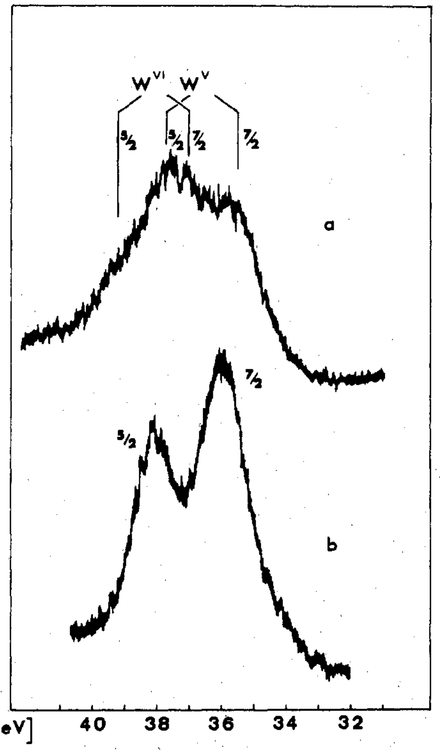

Figure 3. Photoelectron spectra of (a) $[W_4O_8Cl_8(H_2O)_4](HNMe_3)_2{\cdot}2H_2O$ and (b) Rb_2WOCl_5 in the region of the W $4f(^5/_2, ^7/_2)$ doublet.

The spectrum of $Rb_2W^VOCl_5$ showing a normal doublet has been also recorded for comparison. Owing to the poor resolution of the mixed-valence spectrum, only approximate ESCA parameters can be given. Assuming a value of 2.2 eV for the $4f(^7/_2)$–$4f(^5/_2)$ splitting, these are for W^V $4f(^7/_2)$ = 35.5 eV and $4f(^5/_2)$ = 37.7 eV and for W^{VI} $4f(^7/_2)$ = 37.0 eV and $4f(^5/_2)$ = 39.2 eV.

It has been argued by Hush that the appearance of two peaks for an inner-shell transition does not in itself prove the existence of a trapped-valence ground state.[7] This is because the relaxation of the valence electron may occur during the photoionization process. However, in the present case, the existence of distinct W^V and W^{VI} centers is supported by ESR data (see below) and the exchange between them is assumed to be very slow (ca. 10^{-8} s) on the ESCA time scale (10^{-18} s). Thus the appearance of two signals would be quite consistent with a class II trapped-valence system.

Electron Spin Resonance. The ESR spectrum, observed at 77 K on a powder of $[W_4O_8Cl_8(H_2O)_4](HNMe_3)_2{\cdot}2H_2O$, is shown in Figure 4a. It is typical of W^{5+} ions ($S = ^1/_2$; I = O) in a rhombic ligand field. The measured g values g_1 = 1.809, g_2 = 1.777, and g_3 = 1.748 agree with those already published for W^{5+}.[19] The small bump on the low-field side of the spectrum could be due to the hyperfine coupling with the 14% abundant ^{183}W nucleus ($I = ^1/_2$). Assuming that it corresponds to g_1 would give A_1 = 154 G.

As the temperature rises, lines broaden and the spectrum becomes characteristic of an axial form (Figure 4b) before appearing to be wholly isotropic at room temperature (Figure 4c). The two high-field components quickly collapse, suggesting that g_2 and g_3 could be viewed as g_{xx} and g_{yy} ($g_\perp$) and g_1 as g_{zz} ($g_\parallel$). These values are very similar to those observed for $WOCl_5^{2-}$:[20] $g_\parallel$ = 1.804 and $g_\perp$ = 1.752.

The low-temperature spectrum, at 77 K, shows that the unpaired electrons must be localized on separate W nuclei giving a mixed-valence compound containing both W^{6+} and W^{5+} ions. The tungsten ions are surrounded by a rhombic ligand field. This result agrees with the site symmetry determined by x-ray diffraction.

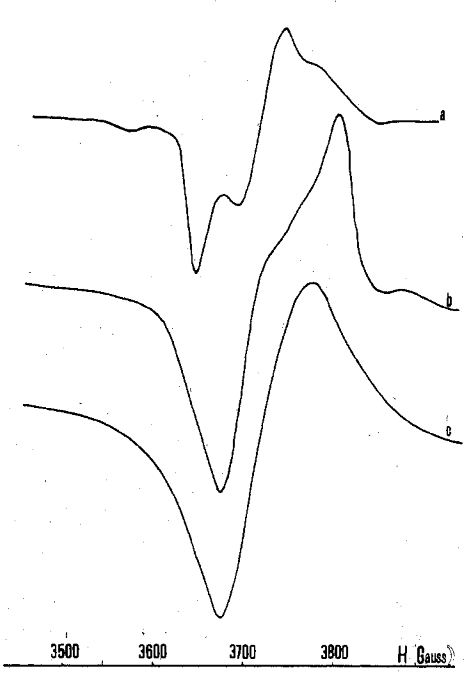

Figure 4. ESR spectra of W^{5+} in a powder of $[W_4O_8Cl_8(H_2O)_4](HNMe_3)_2{\cdot}2H_2O$. Recording temperature: (a) 77 K; (b) 140 K; (c) 300 K.

The line broadening observed when increasing the temperature could be due to an intervalence hopping of the 5d unpaired electrons from a W^{5+} ion to one of its W^{6+} neighbors in the $W_4O_8Cl_8(H_2O)_4^{2-}$ molecule. At 77 K, this hopping frequency must be smaller than the spectrum anisotropy expressed in frequency units, i.e., 2.5×10^8 Hz.

The hopping process is thermally activated and the hopping frequency increases with the temperature. The signal broadens, passing through a maximum (130 G) around −50 °C. We then observe a motional narrowing, and at room temperature, the signal appears to be isotropic. It exhibits a single Lorentzian line 90 G wide. This does not mean that the W^{5+} ions, responsible for the ESR signal, are surrounded by a cubic isotropic ligand field but that the hopping increases the line width beyond the separation of the rhombic components.[21] The hopping frequency is then about 2.5×10^8 Hz at −50 °C when the maximum line width is observed. It must be larger than this value at room temperature.

A more detailed study of the line width variation against temperature would be necessary in order to get a value of the activation energy for the thermal electron transfer. However, at the present stage, it can be noticed that this hopping frequency is much lower than the characteristic frequency associated with molecular vibrations (ca. 10^{13} Hz). Bond lengths have thus time enough to rearrange between two consecutive electronic exchanges and so the title compound is considered as belonging to Robin and Day's class II.

Electronic Spectrum. The electronic spectrum is shown in Figure 5. The two intense bands at 1.54 and 1.82 μm^{-1} may be assigned to intervalence W^V–W^{VI} transitions. Two weak bands are observed as shoulders at 2.58 and 2.28 μm^{-1} (see Figure 5); because of their low intensity, they could be attributed to d–d transitions of W^V. In $WOCl_5^{2-}$, which exhibits C_{4v} symmetry, two d–d bands are observed: $^2B_2 \rightarrow {}^2E$ at 1.42 μm^{-1} and $^2B_2 \rightarrow {}^2B_1$ at 2.52 μm^{-1};[22] however, in the present case the true site symmetry is C_s rather than C_{4v} and this can give rise to a splitting of the ^2E level. So, three d–d bands are expected, as observed for low-symmetry oxovanadium(IV) species.[23] It is thus very likely that a third d–d band is hidden

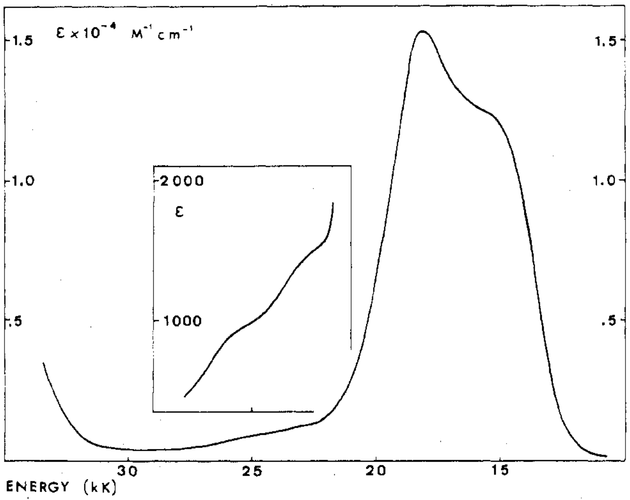

Figure 5. Electronic spectrum of $W_4O_8Cl_8(H_2O)_4^{2-}$ in 12 M HCl. Central portion magnified 5 times in ordinate only.

by the two observed intense intervalence transitions. As far as the latter are concerned, their correct assignment would require the electron correlation knowledge in the mixed-valence complex. Since, on the visible spectroscopy time scale (ca. 10^{-14} s), both d electrons can be considered as localized, one can imagine two possibilities for the ground state, i.e., the two W^V atoms cis or trans with respect to each other. In the present state, further speculation is inappropriate. It is believed that the synthesis of other compounds of the same type but with nonequivalent tungsten atoms will shed some light on this problem. This investigation is now in progress.

Registry No. $[HNMe_3]_2[W_4O_8Cl_8(H_2O)_4]\cdot 2H_2O$, 65027-46-5.

Supplementary Material Available: A listing of structure factor amplitudes (10 pages). Ordering information is given on any current masthead page.

References and Notes

(1) Laboratoire de Chimie des Mêtaux de Transition (Equipe de Recherche Associée au CNRS No. 608).
(2) Laboratoire de Spectrochimie du Solide (Equipe de Recherche Associée au CNRS No. 387).
(3) M. B. Robin and P. Day, *Adv. Inorg. Chem. Radiochem.*, **10**, 247 (1967).
(4) G. C. Allen and N. S. Hush, *Prog. Inorg. Chem.*, **8**, 257 (1967).
(5) N. S. Hush, *Prog. Inorg. Chem.*, **8**, 391 (1967).
(6) B. Mayoh and P. Day, *J. Am. Chem. Soc.*, **94**, 2885 (1972).
(7) N. S. Hush, *Chem. Phys.*, **10**, 361 (1975).
(8) J. P. Launay, *J. Electroanal. Chem. Interfacial Electrochem.*, **54**, 197 (1974).
(9) J. J. Bonnet and Y. Jeannin, *Bull. Soc. Fr. Mineral. Crystallogr.*, **93**, 287 (1970).
(10) (a) D. T. Cromer and J. T. Waber, *Acta Crystallogr.*, **18**, 104 (1965); (b) "International Tables for X-Ray Crystallography", Vol. 3, Kynoch Press, Birmingham, England, 1968, p 215.
(11) D. J. Wehe, W. R. Busing, and H. A. Levy, Document No. TM 229, Oak Ridge National Laboratory, Oak Ridge, Tenn.
(12) ORTEP drawing: C. K. Johnson, Document No. 3794, Oak Ridge National Laboratory, Oak Ridge, Tenn.
(13) A. J. Edwards, *J. Chem. Soc.*, 3714 (1964).
(14) G. Bunzey, J. H. Enemark, J. I. Gelder, K. Yamanouchi, and W. E. Newton, Proceedings of the 2nd International Conference on the Chemical Uses of Molybdenum, Oxford, 1976.
(15) H. T. Evans, *Perspect. Struct. Chem.*, **4** (1971); T. J. R. Weakley, *Struct. Bonding (Berlin)*, **18**, 131 (1974).
(16) P. M. Smith, *Diss. Abstr. Int. B*, **32**, 5136 (1972).
(17) T. Glowiak, M. Sabat, and B. Jezowska-Trzebiatowska, *Acta Crystallogr., Sect. B*, **31**, 1783 (1975).
(18) D. L. Kepert, "The Early Transition Metals", Academic Press, New York, N.Y., 1972, p 289.
(19) B. A. Goodman and J. B. Raynor, *Adv. Inorg. Chem. Radiochem.*, **13**, 136 (1970).
(20) H. Kon and N. G. Sharpless, *J. Phys. Chem.*, **70**, 105 (1966).
(21) R. A. Prados and M. T. Pope, *Inorg. Chem.*, **15**, 2547 (1976).
(22) E. A. Allen, B. J. Brisdon, D. A. Edwards, G. W. A. Fowles, and R. G. Williams, *J. Chem. Soc.*, 4649 (1963).
(23) J. S. Wood, *Prog. Inorg. Chem.*, **16**, 227 (1972), and references therein.

Contribution from the Departments of Mineralogy and Inorganic Chemistry,
University of Marburg, Marburg Lahnberge, West Germany

Presence of a Static Jahn–Teller Distortion in Copper(II) Terpyridine Complexes. 1. Crystal Structure of $Cu(terpy)_2(NO_3)_2$

R. ALLMANN, W. HENKE, and D. REINEN*

Received May 5, 1977

The crystal and molecular structure of diterpyridinecopper(II) nitrate $[Cu(C_{15}N_3H_{11})_2(NO_3)_2]$ has been determined from three-dimensional single-crystal x-ray diffraction data. The green crystals are tetragonal, space group $I4_1/a$ with eight formula units in the unit cell with $a = 12.476$ (6) and $c = 36.284$ (13) Å. The structure was refined to an R of 0.070 for 1931 independent reflections with $F > 1\sigma(F)$. The CuN_6 octahedra are strongly distorted and exhibit approximately orthorhombic symmetry with Cu–N bond lengths of $\simeq 1.99$, 2.08_5, and 2.29 Å, respectively. The geometry is very roughly described as the superposition of a "tetragonal compression" along [001] as the result of the rigid structure of the terpyridine ligands and a "tetragonal elongation" perpendicular to [001] as a consequence of the Jahn–Teller effect. Some of the NCuN bond angles differ distinctly from 90° and the two terpyridine ligands are twisted also but differently in extent. EPR spectroscopic results are included in the Discussion.

Introduction

The σ-antibonding ^2E_g ground state of Cu^{2+} in octahedral coordination is highly Jahn–Teller unstable and leads to strongly distorted ligand environments. In all cases of stochiometric Cu^{2+} compounds known so far the octahedra become tetragonally elongated—with a small orthorhombic component superimposed—if the following conditions are met:[1,2] (a) the octahedral ligands are identical, (b) the octahedral sites of the host lattice are regular when occupied by non-Jahn–Teller ions. The latter condition can be examined by comparison with the stoichiometrically analogous Ni^{2+} or Zn^{2+} compounds, because these ions possess Jahn–Teller stable A ground states in octahedral coordination and ionic radii and electronic configurations similar to Cu^{2+}.

It is possible, however, to force Cu^{2+} into a tetragonally compressed coordination if the host lattice site itself possesses this kind of distortion. Thus in the mixed crystals $Ba_2Zn_{1-x}Cu_xF_6$ compressed CuF_6 octahedra are observed up to $x \simeq 0.3$.[2] The extent of compression, however, is appre-

---

* To whom correspondence should be addressed at Fachbereich Chemie der Universität Marburg, 3550 Marburg Lahnberge, West Germany.

0020-1669/78/1317-0378$01.00/0